Postflight Guidance Accuracy Analysis of Atlas/Centaur/Surveyor Flights

JEROME L. GREENSTEIN*
Convair Division of General Dynamics, San Diego, Calif.

The Atlas/Centaur launch vehicle successfully injected seven Surveyor spacecraft into lunar trajectories with injection errors well below the nominal Surveyor midcourse correction capability of 50 m/sec. The maximum midcourse correction required was 6.4 m/sec and the minimum was 1.2 m/sec. The maximum lunar target miss, prior to the midcourse correction, was 468 km. The minimum was 41 km. An analysis was performed on each flight to separate the injection error into error components due to the guidance hardware, guidance software, and the propulsion system. This was accomplished by reconstructing the guidance trajectory with telemetered guidance sensor data and then comparing this reconstructed trajectory with the nominal trajectory and the trajectory determined from ground tracking data. The injection error results are given in terms of midcourse correction requirements for the guidance hardware, guidance software, and propulsion errors and in terms of trajectory errors for the guidance hardware and propulsion errors. The size of the software error was about as expected. The total guidance hardware error was smaller than expected and was generally equivalent in magnitude to the total software error.

Nomenclature

BET	= best estimated trajectory from Eastern Test Range
DSN	= JPL Deep Space Net
ETR	= Eastern Test Range
GRT	= guidance reconstructed trajectory
FOM	= figure of merit, square root of the trace of the correction velocity covariance matrix
MCR	= midcourse correction requirement
MO	= miss correction only
M + TOF	= miss plus time of flight correction
$\bar{a}$	= acceleration vector
Δ	= operator denoting error term
Γ	= flight-path angle, measured relative to the local horizontal
R_0	= mean equatorial radius
$\bar{r}$	= position vector from earth center
R	= magnitude of position vector
M	= rotation matrix to correct for platform drift
ψ	= range angle in flight plane
t	= time from "go-inertial"
$\bar{v}$	= velocity vector
$\bar{V},\bar{R}$	= vehicle inertial velocity and position vectors determined from tracking data
V	= vehicle inertial velocity magnitude
W	= cross range position measured perpendicular to the reference flight plane
$\dot{W}$	= cross range velocity measured perpendicular to the reference flight plane
X	= range measured along the surface of the earth in the reference flight plane

Subscripts

G	= gravity
m	= vehicle
n	= normal to flight plane
σ	= sigmator quantity
T	= thrust, nongravity forces

Superscript

$(\ )'$	= measured in drifting coordinate system

Introduction

THE Surveyor mission was to soft-land Surveyor spacecraft on the moon to provide basic data for the Apollo program and to contribute new scientific knowledge about the moon.

Seven spacecraft were injected into precise lunar trajectories by Atlas/Centaur launch vehicles. A small midcourse correction was applied to the spacecraft after injection to correct for injection errors and to make adjustments to landing conditions. All seven Surveyors successfully achieved the required injection conditions; the midcourse corrections required were all well below the spacecraft midcourse correction capability of 50 m/sec. Five of the seven spacecraft achieved successful soft landings; two spacecraft developed problems en route and did not soft-land.

The Centaur guidance system, manufactured by Honeywell, consists of a four-gimbal inertial platform stabilized by three single-degree-of-freedom rate integrating gyros (type DGG49D26). The platform contains three mutually perpendicular single-axis hinged pendulum type pulse-rebalanced accelerometers (type DGG177) that measure the thrust and aerodynamic forces acting on the vehicle. A Kearfott digital computer integrates accelerometer pulse data, performs the navigational and guidance equations, and issues steering commands and engine cutoff discretes. The computer memory consists of a 48-track magnetic drum; each track can store sixty-four, 25-bit words. The drum rotates at 100 rps. Critical sensor parameters such as accelerometer bias, scale factor and misalignments, and gyro drift are calibrated prior to launch and used in the navigation equations to correct the accelerometer pulse data.

After each Atlas/Centaur flight, a study was conducted to verify correct performance of the guidance hardware and software and to separate the injection error into individual components of guidance hardware, guidance software, and propulsion error.[1a-1j] A unique computer program was de-

Presented as Paper 68-842 at the AIAA Guidance, Control, and Flight Dynamics Conference, Pasadena, Calif., August 12–14, 1968; submitted August 19, 1968; revision received May 26, 1969. This work was performed under NASA Contract NAS3-8711. The author gratefully acknowledges the assistance provided by M. Winkler, J. Pratt, and T. Van Den Akker toward the development of these analysis techniques. I wish also to gratefully acknowledge the suggestions and encouragement provided by S. Tingley of the NASA Lewis Research Center.

* Design Specialist, Guidance Analysis Group, Launch Vehicles Program. Member AIAA.

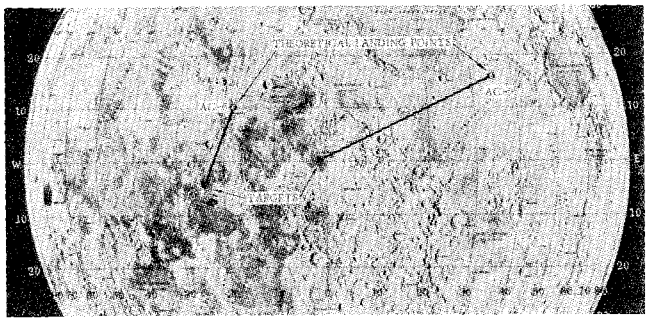

Fig. 1 R&D lunar impacts.

veloped to help separate out these error components. The program used telemetered guidance sensor data as input, recomputing the trajectory measured by the guidance system. The program-computed trajectory was then compared with the desired trajectory and also the trajectory derived from ground tracking data. A discussion of the computer program, postflight analysis procedures, and results achieved are presented in this paper.

Surveyor Injection Accuracy

A summary of the successfully guided flights in order of launch date is given in Table 1. AC-6 and AC-9 were research and development (R&D) flights and did not have actual Surveyor spacecrafts. On early flights, a single burn, direct-ascent trajectory was flown. On later flights, utilizing the restart capability of the Centaur stage, a two-burn trajectory was flown having a parking orbit coast altitude of 90 naut miles and parking orbit coast durations up to 24 min.

Soon after injection, the Surveyor spacecraft was separated from the Centaur stage and tracked by the Jet Propulsion Laboratory (JPL) Deep Space Net (DSN). A midcourse correction was applied to the spacecraft 16 or more hours after injection, to make any desired last-minute changes to the lunar landing point and to correct for target miss due to Atlas/Centaur injection errors. A time-of-flight correction was also required on some trajectories to meet DSN antenna viewing constraints during the soft landing and to adjust the Surveyor main retro burnout velocity.

The target miss for the two R&D flights is shown in Fig 1. AC-6 and AC-9 were the first successful single-burn and two-burn flights, respectively. On these flights no lunar impact was planned. The actual target aimed at was a point in space simulating a target on the moon.

The target miss, prior to the midcourse correction, for the seven actual Surveyor flights is shown in Fig. 2. The maximum target miss, 468 km, occurred on mission C. The minimum, 41 km, occurred on the final flight, mission G. To illustrate the excellent injection accuracy achieved on this final flight, an injection velocity error of 0.1 m/sec corresponds to a target miss of approximately 36 km. The obviously improved accuracy on later missions is explained by continuous improvements that were made in the guidance hardware, guidance software, and in the sensor calibration techniques. Feedback based upon the postflight guidance analysis also resulted in accuracy improvements.

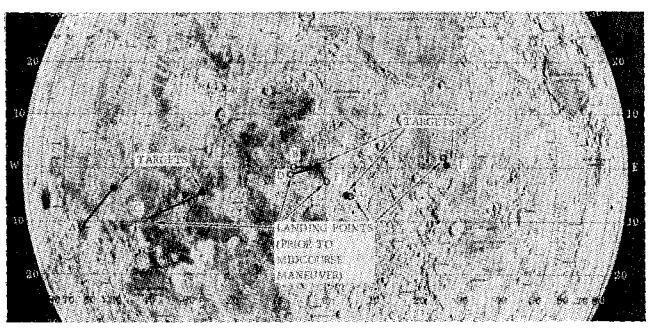

Fig. 2 Surveyor impact points prior to the midcourse correction.

The injection accuracy required of the Atlas/Centaur was that the midcourse correction requirement (MCR) at 20 hr after injection, to correct target miss and time of flight errors, be less than the nominal Surveyor spacecraft correction capability of 50 m/sec. The actual midcourse correction required on each flight was considerably below this. The midcourse corrections required at 20 hr to correct for miss only (MO) and miss plus time of flight (M + TOF) injection errors are shown in Table 1. Also given are the uncorrected target miss distances in kilometers. The first flight, AC-6, had an earlier type accelerometer (DGG116) with large cross-coupling errors. Subsequent flights had the much improved type DGG177. The corrections shown for AC-6 and AC-9 are theoretical only since no corrections were actually applied to the payload.

The largest Surveyor MCR, 6.4 m/sec, occurred on mission A (AC-10). Missions B, E, and G required only 1.2 m/sec.

Postflight Guidance Analysis

Briefly the postflight analysis consisted of:

1) Analog data analysis of a) platform gimbal servo loop data to verify inertial platform stability, b) guidance steering commands and autopilot attitude error signals to verify proper guidance steering loop behavior, c) accelerometer pulse rebalance data to verify stability of accelerometer rebalance loop, and d) power supply stability.

2) Digital computer data analysis as follows:

a) Duplication of the airborne computer calculations on a laboratory computer using telemetered sensor data, to verify correct computer operation and obtain histories of intermediate calculations.

b) Analysis of in-plane and out-of-plane position and velocity steering errors to verify proper performance of guidance steering equations. Also analyzed was the ability of the equations and steering loop to maintain the vehicle thrust vector along the desired velocity-to-be-gained direction.

c) Comparison of guidance and tracking trajectory data to determine injection errors and to separate the injection errors into guidance hardware, software, and propulsion components. When precision tracker data was available, further error separation was attempted in order to determine the individual guidance hardware error sources.

d) Statistical analysis of guidance system calibration history to determine stability of guidance system in terms of shifts in accelerometer scale factor, bias, misalignments, and gyro drifts.

A large effort was directed to item 2c, the error separation. The remainder of this paper is devoted to a further discussion of that portion of the postflight guidance analysis.

Guidance Error Separation

Each major error source had a specific error specification it was required to meet. Although the total injection error on each flight was well below its requirement, it was important to verify by postflight analysis that each individual error source did in fact meet its specification. It was possible that two large errors could have occurred of opposite sign resulting in a cancellation of errors. On subsequent flights cancellation might not have occurred, resulting in a large injection inaccuracy.

Postflight guidance accuracy analysis was desirable for the following additional requirements: 1) determine which errors were most significant and therefore might be candidates for improvements; 2) determine whether any consistent

Table 1 Flight summary

Launch Date	Atlas Centaur No.	Surveyor Spacecraft No.	Surveyor Mission	Launch Azimuth (deg E of N)	Trajectory*	Parking Orbit Length (min)	Lunar Target Lat (deg)	Lunar Target Long (deg)	Target Miss (km)	MCR MO (m/sec)	MCR M+TOF (m/sec)
8/11/65	AC-6	Dyn Model		94.5	DA	0	3.84S	23.65W	454	4.7	13.1
5/30/66	AC-10	SC-1	A	102.3	DA	0	3.25S	43.83W	400	3.8	6.4
9/20/66	AC-7	SC-2	B	114.4	DA	0	0.00	0.67W	141	1.2	1.2
10/26/66	AC-9	Mass Model		99.7	POA	24	0.00	0.67W	1180	6.5	7.5
4/17/67	AC-12	SC-3	C	100.8	POA	22	3.33S	23.17W	468	3.9	6.1
7/14/67	AC-11	SC-4	D	103.8	DA	0	0.58N	0.83W	174	1.5	2.0
9/8/67	AC-13	SC-5	E	79.5	POA	7	0.83N	24.00E	47	0.6	1.2
11/7/67	AC-14	SC-6	F	83.0	POA	13	0.42N	1.33W	126	1.4	2.2
1/7/68	AC-15	SC-7	G	102.9	POA	22	4.95S†	3.88E†	41	0.3	1.2

*DA = Direct ascent (single-burn)
POA = Parking orbit ascent (two-burn)

†After injection, the landing point was moved to 40.9°S Lat and 11.4°W Long

errors occurred which might be biased out; 3) acquire statistical data on accuracy for future missions.

The total injection error was made up of the following three major components: guidance hardware and software errors, and propulsion error.

The hardware errors primarily consisted of uncompensated gyro drifts, shifts in accelerometer scale factor and bias, and uncertainties in platform and accelerometer alignments. The guidance software errors primarily consisted of computation inaccuracies, guidance equation approximations, and extrapolation errors when determining engine cutoff time. Propulsion errors included uncertainties in the Centaur engine shutdown impulse, uncertainties in the spacecraft separation impulse, and dispersions in the coast thrust. (During the parking orbit coast, accelerometer data is not used in order to avoid accelerometer bias errors. Two small engines, with three pounds of thrust each, thrust continuously during parking orbit coast to keep propellants settled.)

The trajectory data available for analysis after each flight normally consisted of:

1) Trajectory computed by airborne computer using guidance sensor data. This trajectory was approximate since it was derived using a simplified gravity model. The limited size and speed of the computer also caused some computation errors.

2) Eastern Test Range best estimated trajectory (BET) derived from ground tracking data. This trajectory normally covered only portions of powered flight and contained some noise and tracker errors, the extent of which depended upon the precision of tracker used (i.e., Glotrac vs radar data). Precision data, from Glotrac, was available on only the initial R&D flights.

3) Surveyor spacecraft lunar transfer orbit based upon 15 or more hours of tracking by the JPL DSN.[2,3a–3c] These data gave the best indication of the spacecraft position and velocity at injection.

4) Nominal simulation of the launch trajectory based as much as possible on actual launch conditions. This gave the injection conditions required to land at the planned lunar target.

In order to accomplish a separation of guidance errors into its major components, it was found a comparison of the preceding data alone was not adequate. For example, to find the total injection error at separation due to guidance hardware error it is necessary to compare the guidance system derived injection conditions with the JPL DSN injection conditions. The only guidance-derived trajectory is generated by the airborne computer, but this trajectory contains software errors and gravity approximations. Therefore, it was found necessary to develop a new computer program that could reconstruct the trajectory based upon guidance sensor data alone. This computer program, called the Guidance-Reconstructed Trajectory (GRT) program, served as the basis for the postflight guidance evaluation of each Surveyor flight and permitted the separation of the guidance error into its three major components of hardware, software, and propulsion error. As shown in Fig. 3, the GRT was compared with the tracking data to obtain the guidance hardware errors, and compared with the nominal trajectory data to find the software and propulsion errors.

Guidance-Reconstructed Trajectory (GRT) Program

During flight, pulses from the three pulse-rebalanced accelerometers and a time standard are summed on a track of the airborne computer drum. This track is called the sigmator track. Therefore, the velocity components are called sigmator velocity ($\bar{v}_\sigma$) and the time called sigmator time (t_σ). Each velocity pulse has a weight of approximately 0.1 fps and each time pulse a weight of 0.77 msec. During flight, at the beginning of each compute cycle, the sigmator velocity and time are sampled and then used in the navigation equations to update the trajectory and generate required steering and engine cutoff commands. Sampling intervals ranged from 1.0 to 1.5 sec. The sampled values of sigmator velocity and time were telemetered. It was this sensor data, stored on tape, that was used as input to the GRT program.

A simplified diagram of the GRT program is shown in Fig. 4. The input is the telemetered sigmator velocity and

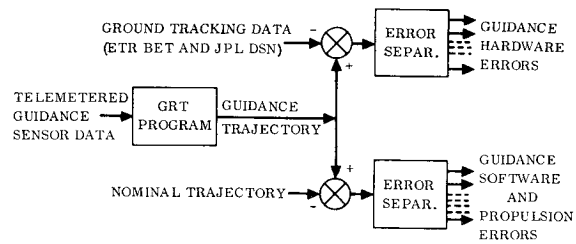

Fig. 3 Trajectory comparison for error separation.

time. The velocity must first be compensated for accelerometer bias, scale factor, and misalignments. The compensations are obtained from prelaunch calibrations of the guidance system. The result $\bar{v}'_T$, called "thrust velocity," is primarily the vehicle velocity due to thrust and aerodynamic forces. The thrust velocity components are then corrected for platform drift. During most flights, torquing was not applied to the gyros to correct for known fixed torque drifts and mass unbalances and thereby keep the accelerometer triad in a fixed orientation during flight. These drifts were calibrated prior to launch and rotational corrections were applied analytically during flight in the airborne computer. Therefore, in the GRT program the thrust velocity $\bar{v}'_T$ is corrected for platform drift to obtain a thrust velocity $\bar{v}_T$ which is in a fixed inertial coordinate system. Since the inertial guidance system does not sense the gravity acceleration, the gravity acceleration is computed and integrated to obtain velocity and position components due to gravity. These are added to the thrust components to obtain the vehicle velocity $\bar{v}_m$ and the vehicle position $\bar{r}_m$. A differentiation of $\bar{v}_T$ is performed to obtain "thrust acceleration" $\bar{a}_T$.

The GRT program performs the navigation equations as they would be performed by an almost unlimited capacity airborne computer, assuming perfect sensor data. The airborne computer also assumes perfect sensor data, but its equations contain integration approximations, a simpler gravity model, truncation and roundoff errors, and time lags. The GRT program, therefore, reconstructs the trajectory as measured by the guidance system.

The GRT program contains various additional capabilities that a) extrapolate trajectory data to engine cutoff times, b) compute orbital parameters at injection, c) compute Centaur engine shutdown impulse, d) compute spacecraft separation impulse, e) substitute a nominal shutdown and separation impulse for the actual impulses, f) substitute a nominal coast thrust for the actual coast thrust, and g) integrate over portions of the flight where data dropouts occur.

Separation of Guidance Hardware Errors

The total guidance hardware error in terms of trajectory errors at injection was determined by comparing the GRT and the DSN injection data. The separation of guidance hardware errors into individual sensor errors such as gyro drift, accelerometer bias, etc. was attempted by comparing the GRT with the ETR BET during powered flight.

Comparison of JPL, DSN, and GRT Data

The JPL DSN data,[2,3a–3e] since it was based upon 15 or more hours of tracking the Surveyor, gave a precise indication of the spacecraft injection state vector. The injection state vector derived from the GRT program contains trajectory errors due to guidance hardware errors. The preflight 3σ estimate of guidance hardware errors was approximately a factor of ten larger than the reported state vector errors of the DSN.[1a–1j] Therefore, the difference between the DSN and the GRT injection state vectors was expected to give a good indication of the guidance hardware injection errors. The resulting errors for each flight are given in Table 2, part A, referenced to flight plane coordinates, X, R, V, Γ, W, $\dot{W}$. The mean and standard deviation of the flight errors (excluding AC-6) are also given in the table.

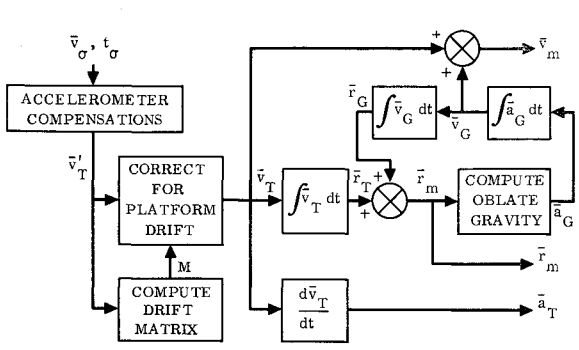

Fig. 4 Guidance-reconstructed trajectory program.

The reference flight plane is defined by the velocity vector $\bar{v}_m$ and the position vector $\bar{r}_m$ at injection, determined by the GRT program. Defining $\bar{V}$ and $\bar{R}$ as the injection state vectors determined from the JPL DSN, then letting

$$\bar{1}_n = \bar{r}_m \times \bar{v}_m / |\bar{r}_m \times \bar{v}_m| \quad (1)$$

$$\Delta\psi \approx \cos(90 - \Delta\psi) = (\bar{R} \times \bar{1}_n / |\bar{R} \times \bar{1}_n|) \bar{r}_m / |\bar{r}_m| \quad (2)$$

$$\Delta X = R_0 \Delta\psi \quad (3)$$

$$\Delta R = |\bar{R}| - |\bar{r}_m| \quad (4)$$

$$\Delta V = |\bar{V}| - |\bar{v}_m| \quad (5)$$

$$\Delta\Gamma \approx \cos(90 - \Delta\Gamma) = (\bar{1}_n \times \bar{V} / |\bar{1}_n \times \bar{V}|) \bar{v}_m / |\bar{v}_m| \quad (6)$$

$$\Delta W = \bar{R} \cdot \bar{1}_n \quad (7)$$

$$\Delta\dot{W} = \bar{V} \cdot \bar{1}_n \quad (8)$$

The largest errors listed in Table 2A were $\frac{1}{2}$ to $\frac{1}{3}$ of the 3σ preflight error estimates. The smaller errors were on the order of the DSN tracking uncertainties.

Since some flights were single-burn and others were two-burn with varying parking orbit lengths, the propagation of sensor errors is different for each trajectory. Therefore, the mean and standard deviations given are not necessarily valid for a whole population of flights but are just provided to give a general indication of the guidance system performance. Similarly, the values given are not necessarily representative of performance expected on other missions.

The magnitude of injection velocity V was consistently high on each flight (mean $\Delta V = 0.44$ m/sec). Excluding the first flight, the largest velocity error was 0.95 m/sec. The position vector R was consistently low on every flight except the last (mean $\Delta R = -0.42$ km). The largest position error was -0.94 km. Flight-path angle Γ was also consistently low (mean $\Delta\Gamma = -0.13$ mrad). On mission C, a small error component is included due to a coast thrust error.

Comparison of GRT and BET Data

After each flight, a best estimated trajectory (BET) was computed by ETR based upon ground tracking of the launch vehicle, primarily during powered flight. The difference between the BET and GRT gave a time history of trajectory error due to tracker and guidance errors.

On early flights, precision tracking equipment (Glotrac) was used that provided an accurate history of the vehicle trajectory (small tracker errors). This permitted an attempt to separate the guidance errors into components of accelerometer bias, scale factor, gyro drift, etc. It is not the intention of this paper to go into much detail on this aspect of the postflight guidance analysis. Some general comments and conclusions are felt necessary to help the novice who might be unwary of the pitfalls involved.

Since the guidance sensor errors are generated in the "thrust" domain, it was decided to subtract out from the BET the gravity component of velocity, $\bar{v}_G$, to perform the error separation on the thrust velocity $\bar{v}_T$. The gravity acceleration was computed from the BET position vector $\bar{r}_m$.

The GRT thrust velocity is obtained by correcting the sigmator velocity, as shown in Fig. 4. The difference between the GRT and BET velocities $\Delta\bar{v}_T$, representing the time history of total guidance sensor error, was fed into an error separation program.

The error separation program, using a weighted least-squares technique, chooses the best combination of sensor errors that, added together, match the time history of total sensor error observed on each trajectory component. A

Table 2 Error separation summary

Error Component	Dynamic Model (AC-6)	Mass Model (AC-9)	Surveyor Mission A (AC-10)	B (AC-7)	C[a] (AC-12)	D (AC-11)	E (AC-13)	F (AC-14)	G (AC-15)	Mean[b]	σ[b]
A. Injection Errors Due to Guidance Hardware											
ΔX (km)	4.50	-1.70	0.24	0.17	4.61	-0.09	-0.09	0.28	0.10	0.44	1.69
ΔR (km)	-2.14	-0.57	-0.41	-0.94	-0.78	-0.34	-0.60	0	0.28	-0.42	0.37
ΔV (m/sec)	1.02	0.55	0.03	0.19	0.95	0.52	0.63	0.38	0.24	0.44	0.27
$\Delta\Gamma$ (mrad)	-0.81	0.04	-0.08	-0.27	-0.49	-0.10	-0.12	-0.02	-0.01	-0.13	0.16
ΔW (km)	0.09	-0.88	0.43	-2.01	-1.81	-0.17	-0.18	2.10	-0.19	-0.34	1.22
$\Delta\dot{W}$ (m/sec)	-1.97	1.94	3.12	-5.87	4.36	-1.57	-0.26	0.23	-0.13	0.23	2.95
B. Engine Shutdown Impulse Errors											
ΔV (m/sec)	0.92	-0.39	1.15	0.72	-0.20	0.16	-0.20	-0.16	-0.23	(c)	(c)
C. MCR Error Separation Summary — M+TOF (M/Sec)											
Hardware	11.8	0.6	2.9	5.0	3.9	1.4	0.7	2.8	1.6		
Software	(c)	3.0	1.7	0.2	2.8	0.6	0.0	2.7	1.1		
Impulse	(c)	2.9	11.0	5.4	1.4	1.2	1.4	1.4	1.8		
Vector Total	13.1	7.5[d]	6.4	1.2	6.1[e]	2.0	1.2	2.2	1.2		
Preflight FOM	26.1	5.0	5.5	7.7	5.6	5.1	6.2	6.0	3.2		

(a) Injection error includes some coast thrust error
(b) AC-6 not included
(c) Not computed
(d) Includes coast thrust error of 1.6 m/sec
(e) Includes coast thrust error of 2.0 m/sec

typical example from the AC-6 flight is shown in Fig. 5. The error on the u component of thrust velocity is shown building up during powered flight to approximately 3 m/sec. Tracker noise is apparent in the curve. The error curve appeared to be due to three sensor error sources: acceleromenter scale factor, accelerometer bias, and platform misalignment. The sum of these errors, in terms of velocity error, closely matched the total sensor error curve.

The error separation technique was successful when large sensor errors occurred. For example, an accelerometer cross-coupling error 11 times the specification value was found on an early flight (this type of accelerometer was later replaced with a much improved model). It was also successful when some of the errors could be deduced from other data to remove the number of possible variables. For example, 1) accelerometer bias errors could bed eterminedfrom free-fall data, 2) plat-form gimbal demodulator outputs indicated a portion of the platform misalignment error, and 3) guidance system calibration history indicated the least stable sensor correction terms.

On most flights, because the sensor errors were small, the error separation program produced results with very large uncertainties. There was poor correlation between the results of the program and errors observed from other data. For example, inertial platform misalignments indicated by platform gimbal error signals did not necessarily show up in the error separation program results.

Some of the problems encountered with the error separation techniques are listed below:

1) Each sensor error tends to vary with flight environment, but was assumed constant in the error separation program. For example, a shift in accelerometer scale factor which might occur prior to or at launch is assumed to remain fixed throughout the powered portion of the flight. This is generally not the case since scale factor can vary as a function of the varying thermal and vibration environment.

2) A large number of possible error sources (approximately 30 in the Centaur guidance system error model) made a choice of specific error cause difficult.

3) There was a similarity of error histories for many of the guidance error sources.

4) Tracker errors were mixed in with the data. There was a similarity of guidance error histories for some of the tracker error sources.

5) High tracking noise and error often occurred during critical portions of the error curves (e.g., during separation of stages after engines have cutoff).

6) There were missing tracking data during critical portions of the error curves (e.g., early and late portions of the flight). In order to distinguish between different types of sensor errors, a total error history during powered flight is very desirable.

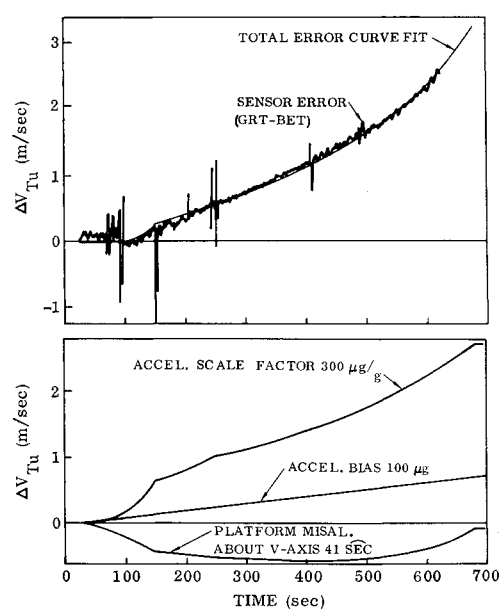

Fig. 5 Sensor error separation.

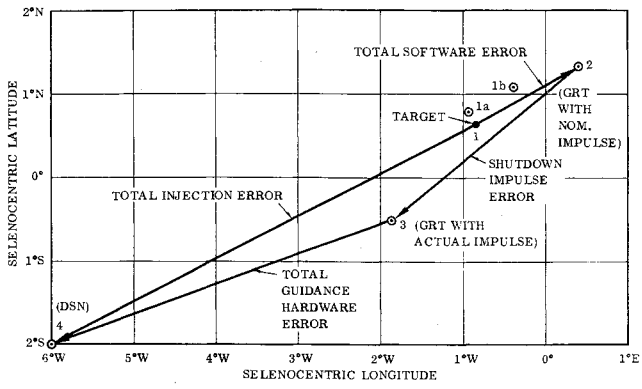

Fig. 6 Mission D lunar impact data.

7) Tracker and guidance measurements occurred in different frames of reference (earth relative vs inertial causing small errors due to gravity model and vehicle angular motions).

8) Errors of opposite sign tend to cancel if their error histories are similar and therefore they might not be apparent in the error separation.

9) Discontinuities in tracking data and error curves occurred when a second tracking transmitter was substituted at a point downrange (called "handover").

Separation of Propulsion Errors

The major source of propulsion error was the Centaur engine shutdown impulse. Two other error sources investigated were the separation impulse and the coast thrust. The propulsion error was determined by comparing the GRT with the nominal trajectory.

Shutdown Impulse

The Centaur engine cutoff criterion was injection energy. When the airborne computer determined that the required energy had been reached, a command was sent to shut off the main Centaur engines. Dispersions occurred in the amount of impulse provided by the engine after the cutoff command was issued. The GRT program extrapolated the thrust velocity to the engine cutoff time. This thrust velocity was differenced with the thrust velocity several seconds after cutoff, and the engine shutdown impulse was thereby calculated. A comparison of the nominal impulse with the flight value gave the impulse error. The impulse error results for each flight, converted into an injection velocity error, are given in Table 2, part B. The value of shutdown impulse had a greater uncertainty on early flights. On mission A, the error was 1.15 m/sec. On later flights, as knowledge of the shutdown impulse improved, the error reduced to values in the range of 0.16–0.23 m/sec.

Separation Impulse

The nominal separation impulse applied to the Surveyor at separation from the Centaur stage was 0.23 m/sec. The GRT program computed the Centaur change in velocity at separation and, assuming conservation of momentum, computed the equivalent spacecraft Δv. No significant spacecraft separation impulse error was found to occur on any of the flights.

Coast Thrust

On two-burn flights, the Centaur was first injected into a nearly circular parking orbit at an altitude of approximately 90 naut miles. Six pounds of thrust was maintained during coast to keep the main engine propellants settled. The sigmator velocity was not accepted by the navigation equations during this period because of the possibility of introducing accelerometer bias errors during a long coast. The guidance equations assumed the coast thrust was nominal since the expected thrust dispersions were less than the expected accelerometer bias errors.

The coast trajectory was reconstructed by the GRT program using the sigmator velocity. This permitted the determination of coast thrust and accelerometer bias errors by comparing the actual and expected coast thrust velocity. Small errors in the nominal value of coast thrust were observed on early flights. On later flights, by changing the assumed nominal value, the error became negligible.

Software Error Separation and MCR Analysis

The total software error was not defineable in terms of injection trajectory components as given for the hardware and impulse errors in Table 2. Most of the errors occurred in terms of injection energy. Some error was due to flying a different trajectory than nominal. The approach used in this study was to define the total software error in terms of the lunar target miss and the 20-hr midcourse correction requirement. The MCR for the guidance hardware error and the MCR for the shutdown impulse error were also determined.

Software Error Separation

The guidance equations, assuming the guidance sensor data to be exact, commanded vehicle steering and engine cutoff to achieve the proper Surveyor injection conditions. If the cutoff conditions commanded by the software were perfect, and were followed by nominal shutdown and separation impulses, then this trajectory, based upon the guidance sensor data, would appear to land precisely at the lunar target. The software error can therefore be established by observing the target miss of the GRT trajectory with a nominal shutdown and separation impulse. The error was also computed in terms of the 20-hr MCR to correct for target miss and time-of-flight errors.

The technique is described by using mission D as an example. Refer to the lunar impact data in Fig. 6. Point 1, shown on the map, was the intended Surveyor landing spot. The guidance trajectory was reconstructed based upon the telemetered sigmator velocity and time, and the prelaunch calibrated sensor compensation values. The trajectory was integrated during powered flight until the last compute cycle prior to engine cutoff. Since engine cutoff does not occur at a computer sampling time, an extrapolation of the trajectory was performed to the time engine cutoff occurred. A nominal shutdown and spacecraft separation impulse was then added to the trajectory, and the trajectory was integrated to the moon to determine the lunar impact, point 2. The separation between the target and point 2 represents the target miss due to the total software error. To correct point 2 back to the target required an MCR of 0.4 m/sec.

The major contributors of software error were then investigated to determine their magnitude. They consisted of:

Targeting error. This was the miss distance of the nominal trajectory and was primarily caused by guidance equation approximations. The nominal trajectory impacted at point 1a on Fig. 6. Therefore the separation between points 1 and 1a corresponds to the software targeting error.

Cutoff extrapolation error. This was due to errors in the cutoff extrapolation equations when determining the desired engine cutoff time. The error, in terms of cutoff energy, was determined and then added to point 1a. The resulting impact was at point 1b.

Truncation error. This error was due to the limited word size of the airborne computer and is a function of the time of powered flight. Since a nominal error was compensated for and near-nominal flight time occurred, no significant truncation error occurred on this flight.

Nonnominal vehicle performance. The error remaining between points 1b and 2 is attributable to vehicle dispersions such as thrust, weight, I_{sp}, etc. In other words, the actual trajectory differs from the one used to derive the guidance steering and cutoff coefficients.

Hardware and Shutdown Impulse MCR

If the actual shutdown impulse is included in the trajectory reconstruction instead of the nominal, point 3 is obtained. The separation between points 3 and 2 represents the shutdown impulse error, and the MCR to correct point 3 back to point 2 was 0.8 m/sec. Point 3 is based upon all of the telemetered sensor data up to the end of the engine thrust decay. Tracking by the JPL DSN gave point 4 as the expected impact point of the Surveyor spacecraft, prior to the midcourse correction. Since the JPL DSN tracker errors were small, the separation between points 4 and 1 represents the total injection error that occurred on the flight. The lunar miss was 174 km, which required a midcourse correction of 1.5 m/sec to achieve landing at the target. The error remaining, which is primarily due to guidance sensor error, is represented by the separation between points 3 and 4. The MCR to correct point 4 back to point 3 was 1.1 m/sec. A time-of-flight correction was also computed for each impact point.

An analysis such as the aforementioned was performed on each Surveyor flight. A summary of the error separation results in terms of the midcourse correction required to correct for both target miss and time-of-flight errors for the guidance hardware, software, and engine shutdown is given in Table 2, part C. The vector sum is also shown, compared with the preflight computed figure of merit (FOM). The FOM is the square root of the trace of the correction velocity covariance matrix derived from a perturbation analysis using one-sigma input errors. It is approximately a 68% probability point.

Sizes of the software MCRs were about as expected and well within specification. Sizes of the guidance hardware MCRs were approximately 50–80% of what was expected based upon the preflight assumed error model. The hardware error model therefore turned out to be overly conservative. The shutdown impulse MCR's were within expected values on the later flights when better knowledge of the nominal value of shutdown impulse became available. On most flights there was a cancelling of error; the vector total was smaller than the largest component. Also on most flights the vector total was considerably smaller than the preflight-computed FOM.

Conclusions

The error separation technique described was successfully used to find the major error components during each flight. In the case of software and propulsion errors, results of the analysis were used to improve the accuracy of subsequent flights. Although it was not done, some consistent hardware errors were observed that could have been compensated for to further improve accuracy. The guidance hardware errors were smaller than expected. Separation of the guidance hardware errors into individual sensor components using the ground tracking data proved considerably more difficult than expected and provided results that were often questionable.

References

[1] a) "Centaur AC-6 Postflight Guidance Analysis," GDC-BTD65-152, Dec. 1965; b) "Centaur AC-7 . . .," GDC-BKM66-030, Nov. 1966; c) "Centaur AC-8 . . .," GDC-BTD66-072, July 1966; d) "Centaur AC-9 . . .," GDC-BKM66-051, Feb. 1967; e) "Centaur AC-10 . . .," GDC-BTD66-109, Aug. 1966; f) "Centaur AC-11 . . .," GDC-BKM67-065, Sept. 1967; g) "Centaur AC-12 . . .," GDC-BKM67-028, July 1967; h) "Centaur AC-13 . . .," GDC-BKM67-081, Dec. 1967; i) "Centaur AC-14 . . .," GDC-BKM68-001, Feb. 1968; and j) "Centaur AC-15 . . .," GDC-BKM68-017, April 1968, Convair, San Diego, Calif.

[2] Thornton, T. H., "The Surveyor I and Surveyor II Flight Paths and Their Determination from Tracking Data," JPL TR-32-1285, Aug. 1968, Jet Propulsion Lab., Pasadena, Calif.

[3] a) "Surveyor III Mission Report—Part I," JPL TR-32-1177, Sept. 1967; b) "Surveyor IV Mission Report—Part I," JPL TR-32-1210, Jan. 1968; c) "Surveyor V Mission Report—Part I," JPL TR-32-1246, March 1968; d) "Surveyor VI Mission Report—Part I," JPL TR-32-1262, Sept. 1968; and e) "Surveyor VII Mission Report—Part I," JPL TR-32-1264, Feb. 1969, Jet Propulsion Lab., Pasadena, Calif.